Received: 16 June 2023 | Revised: 10 August 2023 | Accepted: 11 August 2023

DOI: 10.1002/jcc.27221

RESEARCH ARTICLE

Journal of COMPUTATIONAL CHEMISTRY WILEY

The stability of oxygen-centered radicals and its response to hydrogen bonding interactions

Vasilii Korotenko | Hendrik Zipse

Department of Chemistry, LMU Munich, Munich, Germany

Correspondence
Hendrik Zipse, Department of Chemistry, LMU Munich, Butenandtstrasse 5-13, 81377 Munich, Germany.
Email: zipse@cup.uni-muenchen.de

Funding information
Deutsche Forschungsgemeinschaft, Grant/Award Number: SFB 1309 (PID 325871075)

Abstract

The stability of various alkoxy/aryloxy/peroxy radicals, as well as TEMPO and triplet dioxygen ($^3O_2$) has been explored at a variety of theoretical levels. Good correlations between RSE_{theor} and RSE_{exp} are found for hybrid DFT methods, for compound schemes such as G3B3-D3, and also for DLPNO-CCSD(T) calculations. The effects of hydrogen bonding interactions on the stability of oxygen-centered radicals have been probed by addition of a single solvating water molecule. While this water molecule always acts as a H-bond donor to the oxygen-centered radical itself, it can act as a H-bond donor or acceptor to the respective closed-shell parent.

KEYWORDS
ab initio calculations, hydrogen abstraction, hydrogen bonding, isodesmic equations, radicals, thermodynamic stability

1 | INTRODUCTION

Oxygen-centered radicals play a central role in radical reactions as diverse as the autoxidation of lipids and its inhibition through antioxidants, the cumol hydroperoxide process for the production of acetone and phenol, or the reduction of ribonucleotides by class I ribonucleotide reductase.[1–8] The radicals involved in these reactions vary largely in terms of their kinetic and thermodynamic properties (Figure 1). On the high-activity end of the scale, we may find the hydroxyl radical (•OH, **1**), whose often very short lifetime in solution-phase experiments is tightly connected to its low thermochemical stability. Oxygen-centered radicals of intermediate stability are those derived from phenoxy radical (**2**), either in the context of the antioxidative activity of phenols such as α-tocopherol (**3**), or in enzyme-mediated reactions involving tyrosyl radicals (**4**).[9–11] On the low-activity end, we can find nitroxyl radicals such as (2,2,6,6-tetramethylpiperidin-1-yl)oxy radical (TEMPO, **5**), whose kinetic and thermochemical stability is high enough to allow bottling and shipping at ambient temperature. The electronic structure of oxygen-centered radicals is typically characterized by the presence of two lone pairs at the spin-carrying oxygen atom as shown in Figure 2. Interactions between oxygen-centered radicals and their condensed-phase environments depends, among others, on specific interactions of these lone pair orbitals and the unpaired spin with suitable interaction partners. Three specific types of interaction have to be anticipated based on earlier precedent as shown in Figure 2 for water as a molecular probe. These include: (a) hydrogen bonding interactions, where one of the RO• radical lone pair orbitals acts as the hydrogen bond acceptor; (b) single-electron hydrogen bond (SEHB) interactions involving the RO• radical SOMO and the σ*(OH) orbital of water; and (c) 2c3e "hemibond" interactions[12] between the RO• radical SOMO and one of the water lone pair orbitals. In the following, we analyze the impact of these interactions on the thermodynamic stability of oxygen-centered radicals RO• as a function of the substituent R.

2 | METHODS

2.1 | Methodological considerations

The thermodynamic stability of O-centered radicals can be characterized by the O—H bond dissociation energy (BDE(OH)) of the

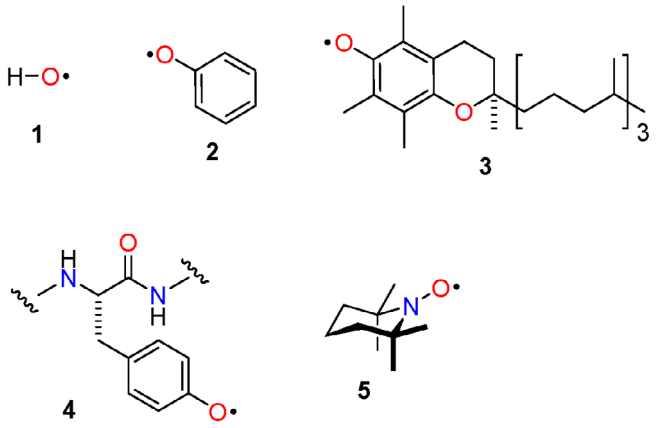

FIGURE 1 O-Centered radicals involved in common radical reactions: hydroxyl radical (**1**), phenoxy radical (**2**), α-tocopheryl radical (**3**), tyrosyl radical (**4**), and TEMPO radical (**5**).

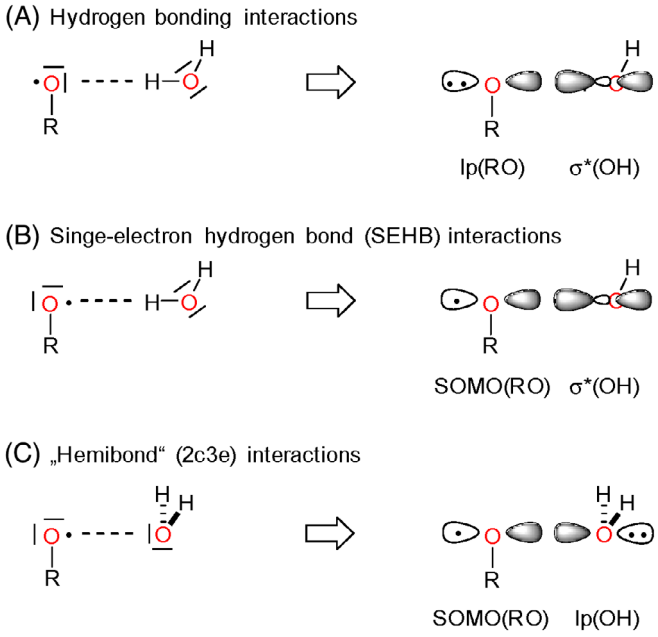

FIGURE 2 Possible interaction types between oxygen-centered radicals RO• and a water molecule.

respective alcohols as defined in reaction 1 in Figure 3, larger values indicating thermochemically less stable radicals. Variations of BDE(OH) values can conveniently be expressed relative to a common reference system such as hydroxyl radical (**1**) through the formal hydrogen atom transfer reaction shown in reaction 2 in Figure 3. The reaction enthalpy at 298.15 K calculated for this isodesmic hydrogen transfer reaction is sometimes referred to as the radical stabilization energy (RSE) of radical RO• as it reflects, to a certain extent, the influence of substituent R on the properties of radical RO•. Combination of these RSE values with the experimentally determined BDE value of water[13] of BDE(OH, **1H**) = +497.3 ± 0.1 kJ mol^{-1} as expressed in Equation (1) provides an indirect and accurate way for the determination of BDE(OH) values in alcohols ROH.[14–20]

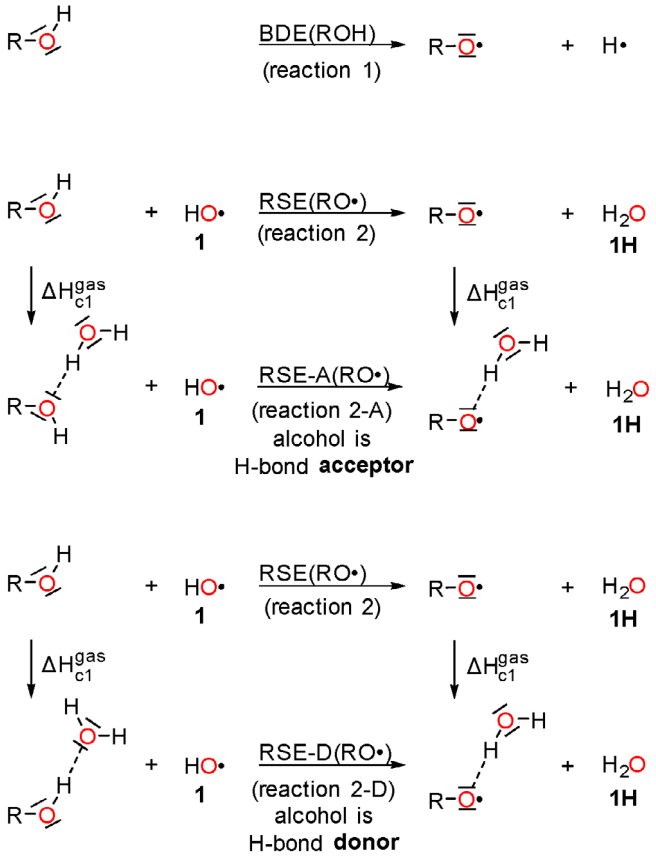

FIGURE 3 Interaction of an explicit water molecule with oxygen-centered radicals RO• and the respective parent alcohols ROH.

$$\mathrm{BDE(RO-H)} = \mathrm{RSE(RO\bullet)} + \mathrm{BDE_{exp}(HO-H)} \quad (1)$$

$$\Delta\mathrm{RSE} = \mathrm{RSE-A/D(RO\bullet)} - \mathrm{RSE(RO\bullet)} =$$

$$= \Delta\mathrm{H^{gas}_{c1}(RO\bullet)} - \Delta\mathrm{H^{gas}_{c1}(ROH)} \quad (2)$$

$$\mathrm{BDE-A/D(RO-H)} = \mathrm{BDE(RO-H)} + \Delta\mathrm{RSE} \quad (3)$$

Aside from serving as a general indicator of radical stability, the BDE(OH) values also provide the basis for assessing the thermodynamics of hydrogen transfer reactions between O-centered radicals and hydrogen atom donors. The experimental determination of BDE(OH) values has only in selected cases been possible with "chemical accuracy," which is often taken to be at the 1 kcal mol^{-1} (or 4 kJ mol^{-1}) limit. In order to provide accurate values for a broader range of systems, efforts have in recent years been undertaken to identify theoretical methods for the accurate calculation of bond dissociation energies.

2.2 | Theoretical methods

The theoretical methods used in these types of studies range from DFT-based methods (for extended systems),[21–24] wavefunction-based

methods involving perturbation theory such as the ROMP2 (FC)/6-311+G(3df,2p) approach,[12,18] double-hybrid functionals such as B2-PLYP,[25,26] all the way to highly elaborate compound schemes such as G3(MP2)-RAD,[14–20,27–32] G3B3,[33,34] CBS-QB3,[35] or the Weizmann-family[36] of methods. More recently, the DLPNO-CCSD(T) method for open-shell systems has emerged as an additional tool for the accurate description of larger radicals, in particular when combined with the complete basis set (CBS) extrapolation scheme.[37–39] The underlying geometries employed in the above-mentioned theoretical approaches are often optimized using hybrid DFT methods. The compound G3B3 method, for example, employs geometries optimized at the (U)B3LYP/6-31G(d)[40–42] level of theory. Particularly for larger molecular systems, the geometries optimized with or without corrective terms for London dispersion interactions (e.g., the D3 corrections parameterized by Grimme et al.)[43,44] may differ considerably. Preliminary calculations of selected RO• radicals furthermore indicated that consistent structural data require a basis set at least as large as 6-31+G(d,p) (see Supporting Information for further details). The subsequent results are therefore based on geometries optimized at the (U)B3LYP-D3/6-31+G(d,p) level of theory.

2.3 | Conformational analysis

The initial structures of molecular complexes were generated randomly using the "kick" algorithm.[45] Geometry optimizations have been performed using the (U)B3LYP hybrid functional, either alone or complemented by the D3 dispersion correction.[44] The 6-31G(d) and 6-31+G(d,p) all electron basis sets have been used for all elements. Frequency calculations have been carried out to verify that the optimized structures are true minima. Thermochemical corrections to H^{gas} and G^{gas} at 298.15 K were calculated using the rigid rotor/harmonic oscillator model.[46] The symbol (^{gas}) denotes a gas phase standard state of 1 atm. The individuality of the found conformers was confirmed using an energy criterion $\Delta E_{tot} > 10^{-7}$ Hartree[47] and comparing geometries by distances between each atom and the centroid point.[48] A detailed description of both algorithms can be found in the Supporting Information.

2.4 | Experimental data

Table 1 contains RSE and BDE(OH) values for systems selected such that they represent the three most relevant classes of substituents in O-centered radicals: (a) radicals with alkyl substituents attached to the spin-bearing oxygen atom such as methoxy radical (**6**); (b) radicals with π-systems attached to the radical center as is the case in phenoxy radical (**2**) or formyloxy radical (**20**); and (c) radicals with lone-pair donors attached to the radical oxygen as is found in peroxy radicals or in nitroxyl radicals such as TEMPO (**5**). The last column in Table 1 collects experimentally determined BDE(OH) values together with the respective RSE(RO•) values obtained according to reaction 2 in Figure 3. In several cases, data from different experimental sources have been considered, and the currently most accurate recommended value is labeled in bold. Wherever available, data form the *Active Thermochemical Tables* (ATcT) have been employed.[13] The O—H bond enthalpy in water of BDE(OH) = 497.3 ± 0.3 kJ mol^{-1} represents the upper bond enthalpy limit and thus an important reference for all other systems considered here.[13,52] For the O—H bond enthalpy in *t*-BuOH (**7H**) photoelectron spectroscopy measurements[50] yield a value of 444.9 kJ mol^{-1}, while thermochemical measurements yield a slightly larger value of 446.8 kJ mol^{-1}.[52] The BDE(OH) for methanol (**6H**) has an ATcT value of 440.4 kJ mol^{-1}, which is closely matched by data from photoelectron spectroscopy.[50] The O—H bond enthalpy in ethanol (**9H**) at BDE(OH) = 440.4 ± 0.5 kJ mol^{-1} is practically identical to that in methanol, which implies only a minor effect through the different alkyl substituents.[13,53] Stabilizing effects through further elongations in the alkyl chain remain moderate as can be seen from BDE(OH) = 432.3 kJ mol^{-1} for *n*-butanol (**11H**),[55] as are the effects of benzylic substituents as in benzyl alcohol (**8H**) with BDE(OH) = 442.7 kJ mol−1[53] or in cumyl alcohol PhC(CH$_3$)$_2$OH (**10H**) with BDE(OH) = 438.2 kJ mol^{-1}.[54] The most accurate gas phase measurements for phenol (**2H**) have been reported by Ashfold and coworkers at 0 K.[64] As stated previously,[15] the addition of thermal corrections (0.6 kJ mol^{-1}) to the experimentally determined RSE values yields the most accurate values of BDE(OH) = 365.0 kJ mol^{-1} for phenol (**2H**) and BDE(OH) = 356.6 kJ mol^{-1} for *para*-methylphenol (**14H**). Combination of the value for **2H** with known substituent effects[56,65] we obtain reference BDE(OH) values for substituted phenols X-PhOH with X = NH$_2$ (324 ± 13) and X = NO$_2$ (390 ± 8). The O—H bond energies in hydroperoxides are quite similar to those in phenols, the value for the parent hydrogen peroxide (H$_2$O$_2$, **13H**) amounting to BDE(OH) = 365.7 ± 0.2 kJ mol^{-1} and that for methylhydroperoxide **15H** being only slightly lower at BDE(OH) = 358.4 ± 0.7 kJ mol^{-1}. This latter value is closely similar to a recent comparative analysis of alkylhydroperoxides,[61] but somewhat lower than earlier estimates based on gas phase kinetics measurements.[59,60] The currently available BDE(OH) data for PhCH$_2$OOH (**16H**) of BDE(OH) = 365 kJ mol^{-1} and *t*-BuOOH (**17H**) of BDE(OH) = 352.3 ± 8.8 kJ mol^{-1} are somewhat less accurate and have also seen less attention than most other systems in Table 1.[58,60] For TEMPO-H (**5H**), we adopt the currently recommended BDE(OH) value in heptane solution of 293.2 kJ mol^{-1}.[62,63] Triplet dioxygen (^{3}O$_2$, **19**) is also included here as an important oxygen-based radical, despite the fact that it carries a triplet ground state and thus differs from all other systems in Table 1. It is nevertheless included here due to its frequent involvement in oxidation reactions and its debatable role in direct hydrogen atom abstractions from hydrocarbon substrates. The rather low value of BDE(OH) = 205.8 kJ mol^{-1} in radical HOO• (**13**) already implies that direct hydrogen atom abstractions from hydrocarbon substrates by ^{3}O$_2$ are thermochemically rather unfavorable.

TABLE 1 RSE(RO•) values for selected O-centered radicals (in kJ mol^{-1}) calculated at various levels of theory together with available experimental data (and the associated BDE(O—H) data) ordered by experimental BDE(RO•) values.

	RSE(RO•)									BDE(RO•)
	DFT[a]	(U)B2PLYP[b,c]		DLPNO-CCSD(T)[b,c]			G3B3-D3			
Radical		TZ	QZ	TZ	QZ	CBS	[b]	[d]	Exp.	Exp.
HO• (**1**)	0.0	0.0	0.0	0.0	0.0	0.0	0.0	0.0	0.0	+497.3 ± 0.1[13] +497.1 ± 0.3[49]
HC(O)O• (**20**)	−35.2	−40.0	−43.3	−14.3	−18.6	−20.9	−30.2	−27.6	−28.4 ± 0.6	+468.89 ± 0.56[13]
t-Bu-O• (**7**)	−57.7	−49.9	−52.3	−42.8	−45.4	−46.7	−47.2	−47.7	−52.4 ± 2.8	+444.9 ± 2.8[50,51] +446.8 ± 4.2[52]
$PhCH_2O$• (**8**)	−65.0	−57.3	−59.2	−48.4	−50.8	−52.2	−54.8	−55.5	−54.6 ± 8.8	+442.7 ± 8.8[51,53]
CH_3O• (**6**)	−65.3	−58.6	−60.3	−53.4	−55.5	−56.6	−55.3	−55.8	−56.9 ± 0.3	+440.4 ± 0.3[13] +440.2 ± 3.0[51,52] +437.7 ± 2.8[50]
CH_3CH_2O• (**9**)	−66.6	−58.7	−60.4	−52.5	−54.6	−55.7	−57.5	−54.8	−56.9 ± 0.5	+440.4 ± 0.5[13] +441.0 ± 5.9[51,52] +438.1 ± 3.3[50]
$PhC(CH_3)_2O$• (**10**)	−58.1	−50.5	−53.2	−40.9	−43.7	−45.1	−45.9	−47.8	−59.1 ± 1.0	+438.2 ± 1.0[51,54]
n-Bu-O• (**11**)	−66.8	−59.1	−61.1	−52.2	−54.5	−55.7	−52.9	−55.3	−65.0	+432.3[55]
p-nitro-PhO• (**12**)	−114.5	−97.7	−100.8	−100.8	−104.3	−106.1	−113.4	−106.0	−107 ± 8	+390 ± 8[15,56] +396 ± 8[56]
HOO• (**13**)	−134.4	−133.7	−135.8	−124.9	−128.1	−129.6	−129.2	−129.6	−131.6 ± 0.2	+365.7 ± 0.2[13]
PhO• (**2**)	−132.9	−114.2	−117.7	−116.3	−121.0	−123.6	−121.1	−121.6	−132.3 ± 0.5	+365 ± 0.5[15] +371.3 ± 2.3[56] +367.1 ± 0.9[13] +362.7 ± 3.0[57]
$PhCH_2$-OO• (**16**)	−139.0	−136.4	−140.4	−122.1	−125.9	−128.0	−126.5	−131.5	−132.3	+365[58]
CH_3OO• (**15**)	−141.8	−139.4	−142.4	−128.9	−132.8	−134.7	−133.0	−135.8	−138.9 ± 0.7	+358.4 ± 0.7[13] +370.3 ± 2.1[51,59] +367.3 ± 4[60] +357 ± 5[61]
p-methyl-PhO• (**14**)	−141.3	−122.5	−126.3	−122.5	−127.6	−130.5	−128.8	−129.3	−140.7 ± 0.6	+356.6 ± 0.6[15] +363 ± 4[57]
t-Bu-OO•	−148.5	−145.6	−149.1	−132.7	−136.8	−138.7	−140.8	−141.5	−145 ± 8.8	+352.3 ± 8.8[51,60]

TABLE 1 (Continued)

Radical	RSE(RO•)							BDE(RO•)	
	DFT[a]	(U)B2PLYP[b,c]		DLPNO-CCSD(T)[b,c]			G3B3-D3		Exp.
		TZ	QZ	TZ	QZ	CBS	[b]	[d]	
(17)									
p-amino-PhO• (18)	−168.8	−152.2	−156.1	−143.9	−149.3	−152.4	−153.3	−153.8	−173 ± 13	+324 ± 13[15,57] +331 ± 13[57]
TEMPO (5)	−208.0	−206.4	−210.9	−185.1	−191.7	−195.4	−198.0	−198.4	−204.1 ± 0.4	+293.2 ± 0.4[62] +291.2[63]
$^3O_2$ (19)	−274.6	−291.7	−294.4	−283.8	−288.0	−290.1	−289.1	−289.2	−291.5 ± 0.2	+205.8 ± 0.27[13]
MSE	−2.8	3.3	0.4	12.1	8.3	6.4	5.4	5.2		
MUE	5.5	6.6	7.0	12.1	8.3	6.4	5.4	5.3		
R^2	0.9956	0.9823	0.9830	0.9906	0.9926	0.9936	0.9938	0.9935		

[a]"DFT"—(U)B3LYP-D3/6-31+G(d,p).
[b]Using (U)B3LYP-D3/6-31+G(d,p) optimized geometries.
[c]"TZ, QZ"—cc-pVTZ, cc-pVQZ.
[d]Using (U)B3LYP-D3/6-31G(d) optimized geometries.

3 | RESULTS

3.1 | Influence of theoretical methods

Basis set effects were studied for (U)B2PLYP and DLPNO-CCSD(T) calculations using (U)B3LYP-D3/6-31+G(d,p) optimized geometries. The two-point (cc-pVTZ and cc-pVQZ) extrapolation strategy was employed for DLPNO-CCSD(T) calculations to estimate the CBS limit.[37,38] In general, changing the basis set from cc-pVTZ to cc-pVQZ in case of both (U)B2PLYP and DLPNO-CCSD(T) makes the RSE as defined by reaction 2 in Figure 3 slightly more negative and also leads to a small improvement of the correlation coefficient with experimental values R^2 (Table 1). The rather moderate magnitude of these effects suggests that calculations with basis sets of quadruple zeta quality may only be required in exceptional cases. In Table 1, it can be seen that DLPNO-CCSD(T)/CBS and G3B3-D3 results are quite similar for most systems, the largest difference (−20.9 vs. −27.7 kJ mol^{-1}) being that for formyloxy radical (**20**). Correlations for the RSE values calculated at G3B3-D3 and DLPNO-CCSD(T)/CBS levels with the corresponding experimental data is shown in Figure 4. Both have positive mean signed errors (MSE) and mean unsigned errors (MUE) of almost identical magnitude, which implies that the calculated radical stabilities are systematically smaller than experimental values. Perusal of Table 1 indicates this to result mainly from the values for the four phenoxy radicals **2**, **12**, **14**, and **18**. The economical (U)B3LYP-D3/6-31+G(d,p) method employed for geometry optimization shows, in comparison, an impressively good correlation.

3.2 | The stability of alkoxy radicals in the absence of intermolecular interactions

The stabilities of oxygen-centered radicals as collected in Table 1 and shown graphically in Figure 4 depend significantly more on the attached substituents than carbon- or nitrogen-centered radicals. The underlying mechanisms for these substituent effects have been discussed earlier and will therefore be reiterated here only briefly.[66,67] Alkyl substituents are moderately stabilizing with RSE values around −62 ± 5 kJ mol^{-1} through hyperconjugative interactions between the oxygen-based SOMO and the neighboring C—C and C—H bonds. The latter appear somewhat more effective as can be seen from the stability difference between the methoxy and *tert*-butoxy radicals (**6** vs. **7**). The stability of aryl- and acyloxy-radicals varies widely as a function of the structure of the attached π-system. On the low stability side, this includes the formyloxy radical (**20**) with RSE(**20**) = −28.4 kJ mol^{-1}, whose delicate electronic structure has been noted in earlier theoretical studies.[68] The phenoxy radical **2** is, in comparison, much more stable at RSE(**2**) = −132.3 kJ mol^{-1}, and displays an impressive stability variation of more than 50 kJ mol^{-1} between its 4-nitro- and 4-amino-substituted variants (**12** vs. **18**). Peroxy radicals are similarly stable as phenoxy radical **2**. For the alkyl-substituted cases **15**, **16**, and **17** included here we note that their stability is only moderately higher as compared with the parent HOO• radical at RSE

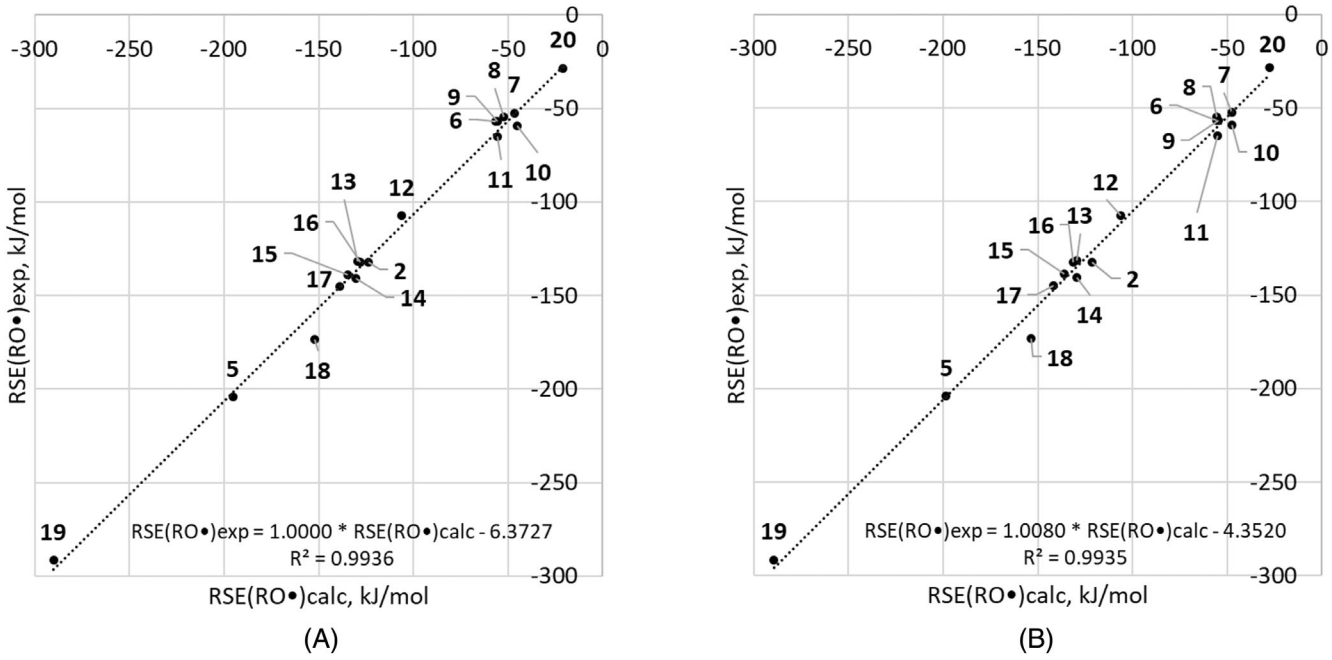

FIGURE 4 Correlation plots for (A) DLPNO-CCSD(T)/CBS//(U)B3LYP-D3/6-31+G(d,p) and (B) G3B3-D3.

(**13**) = −131.6 kJ mol^{-1}. Nitroxyl radicals such as TEMPO are, in comparison, significantly more stable at RSE(**5**) = −204 kJ mol^{-1}, which illustrates the superior ability of amino- as compared with alkoxy-groups to act as electron donors. The even higher stability of triplet dioxygen at RSE(**19**) = −291.5 kJ mol^{-1} simply documents the unique electronic structure of this system,[69] that cannot (and should not) be compared directly with all other O-centered (doublet state) radicals in this study.

3.3 | The effects of monosolvation

The principal interaction modes of explicit water molecules with oxygen-centered radicals RO• have already been detailed in Figure 2. When assessing the impact of these interactions on radical stability as defined earlier in reaction 2 in Figure 3, we also have to decide on the interaction of water with the parent alcohols. One obvious interaction scheme is shown in reaction 2-A in Figure 3, where the parent alcohols act as hydrogen-bond acceptors in very much the same way as the oxygen-centered radicals. RSEs calculated with these interaction types will be designated "RSE-A" and reflect, in addition to the influences of substituent R, the change in hydrogen bond strength to the alcohol oxygen on radical formation. Alternatively, the parent alcohols may also act as a hydrogen-bond donor to the water molecule probe, while the oxygen-centered radical remains to act as a hydrogen-bond acceptor as expressed in reaction 2-D in Figure 3. RSEs calculated according to this latter definition will be designated "RSE-D." In the following, we will first analyze how RSE-A values differ from the gas phase values presented before in Table 1.

The smallest system, where the influence of water complexation can be explored, is the H_2O/HO• radical reference system itself (i.e., R═H in Figure 2). This involves the water dimer on the reactant side, whose hydrogen-bound structure has been studied in large detail experimentally as well as theoretically.[70–72] Whether or not minima other than the structure shown in Figure 5 exist on the potential energy surface depends largely on the theoretical method.[73] At the B3LYP-D3/6-31+G(d,p) level employed here only one true minimum can be located for the water dimer. This minimum is characterized by a hydrogen bonding distance of 191.2 pm. Three true minima are found for the complex of hydroxyl radical **1** with water at the UB3LYP-D3/6-31+G(d,p) level.[74] In the energetically most favorable structure the HO• radical acts as hydrogen bond donor, while the roles are reversed in the second-best structure **1a_2** located 8.0 kJ mol^{-1} higher in energy (DLPNO-CCSD(T)/CBS results).[75–79] This latter structure corresponds to the hydrogen bonding situation shown in Figure 2a and is characterized by a hydrogen bonding distance of 203.2 pm. The energetically least stable minimum corresponds to a "hemibond" structure **1a_3** best described by the orbital interaction described before in Figure 2c and is located 13.0 kJ mol^{-1} higher. Concentrating on water complex **1a_2** with the hydrogen-bonding pattern shown in Figure 2a, a radical stabilization energy of RSE-A(**1a**) = +4.1 kJ mol^{-1} is obtained at the DLPNO-CCSD(T)/CBS level of theory. By definition, the corresponding RSE value in the absence of hydrogen bonding interactions with water is 0.0 kJ mol^{-1}, and we may thus conclude that hydrogen-bond formation to the oxygen atom of the HO• radical is destabilizing by +4.1 kJ mol^{-1}. From the geometrical data and the ESP plots for the water complexes **1Ha** and **1a_2**, as well as the SD plot for **1a_2** we can see that the underlying hydrogen bonding interactions correspond to those expected from

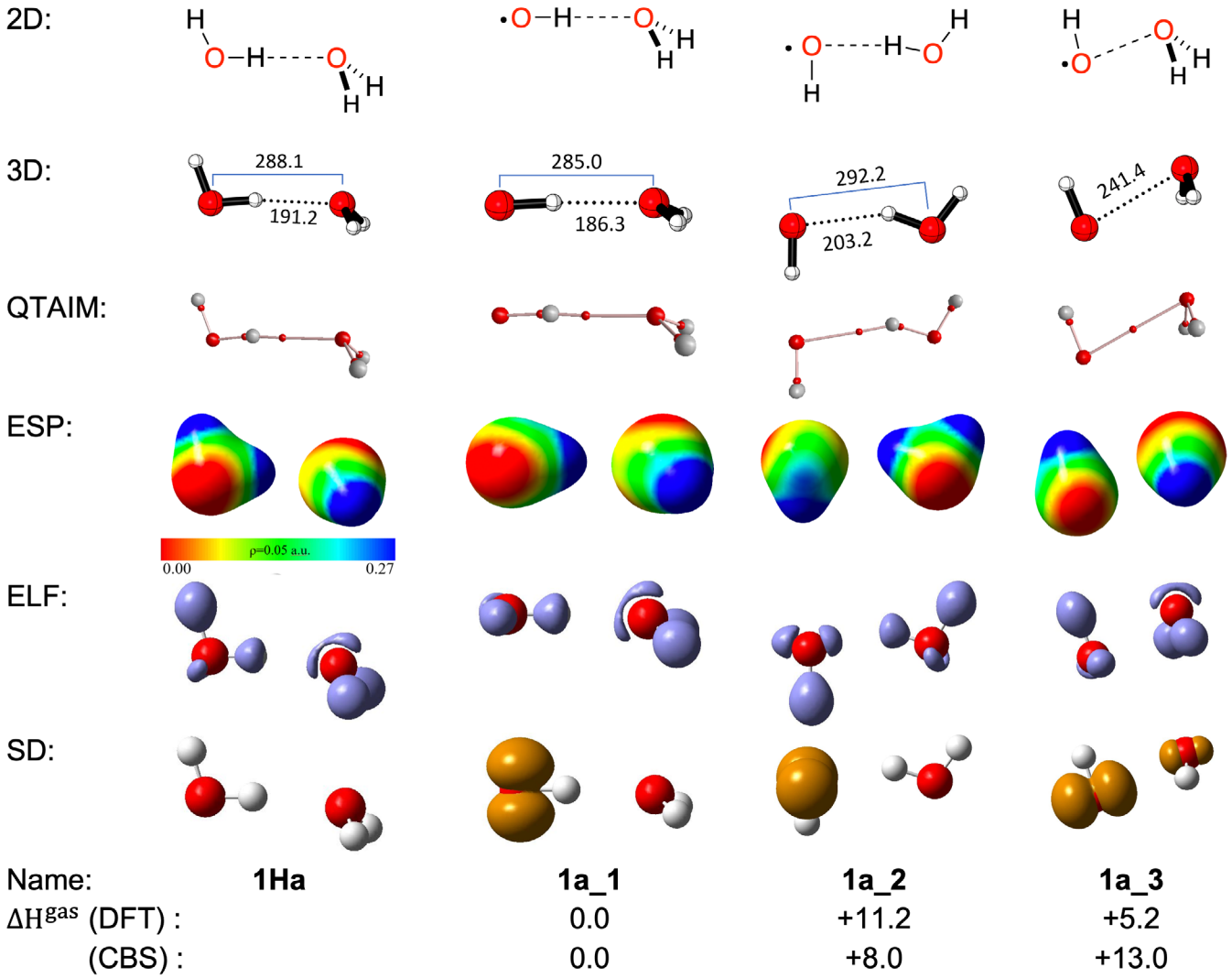

FIGURE 5 2D- and 3D-structures, quantum theory of atoms in molecules (QTAIM), electrostatic potential (ESP), electron localization function (ELF = 0.90 a.u.), spin density (SD = 0.01 a.u.) for water dimer **1Ha** and the water complexes of hydroxyl radical **1a_1**–**1a_3**. For the latter three complexes relative enthalpies ΔH^{gas} (kJ mol^{-1}) calculated at the (U)B3LYP-D3/6-31+G(d,p) (DFT) and DLPNO-CCSD(T)/CBS (CBS) levels are also given.

the principal interaction types presented in Figure 2. This is also supported by NBO analysis of the hydrogen bonding interaction strengths of these systems (see Supporting Information).

Analysis of the energetically best water complexes of all other radicals studied here shows that the hydrogen-bonding pattern described by Figure 2a is present in all of these. Interactions of types (b) and (c) can also be identified for some of the radicals, but these are systematically less stable and thus have a comparatively low Boltzmann population with little impact on the calculated RSE values. Further structural analysis of the water complexes of O-radicals and their parent alcohols indicates that more than one contact typically exists between the complexation partners. These can be C-H···O$_W$,[78,80,81] Ar···H$_W$[78,82] and other weak "secondary" intermolecular interactions,[83] or a second hydrogen bond (as in the case of peroxy radicals and the corresponding peroxide parents, see below). These additional interactions are stabilizing in nature and thus influence both the water/substrate complexation energies and their structural characteristics. As a consequence, the water/substrate complexation energies show only poor correlations with single structural parameters such as hydrogen bond distances.

The molecular orbitals of phenoxy radical **2** shown as an example in Figure 6 allow, in combination with the associated molecular electrostatic potential (ESP), for a better understanding of the intermolecular interactions. The 24α and 24β (HOMO) orbitals have a similar shape and contribute to the electron density on the oxygen atom along the aromatic ring plane, to which the 25α (SOMO) and 25β (LUMO) orbitals show a perpendicular orientation.

Since there is no electron in the LUMO, this leads to the formation of two more negative ESP-regions on oxygen favorable for hydrogen bonding interactions. All oxygen-centered radicals studied here have a similar electronic structure at the radical center. The second effect, which can affect the charge distribution on the radical

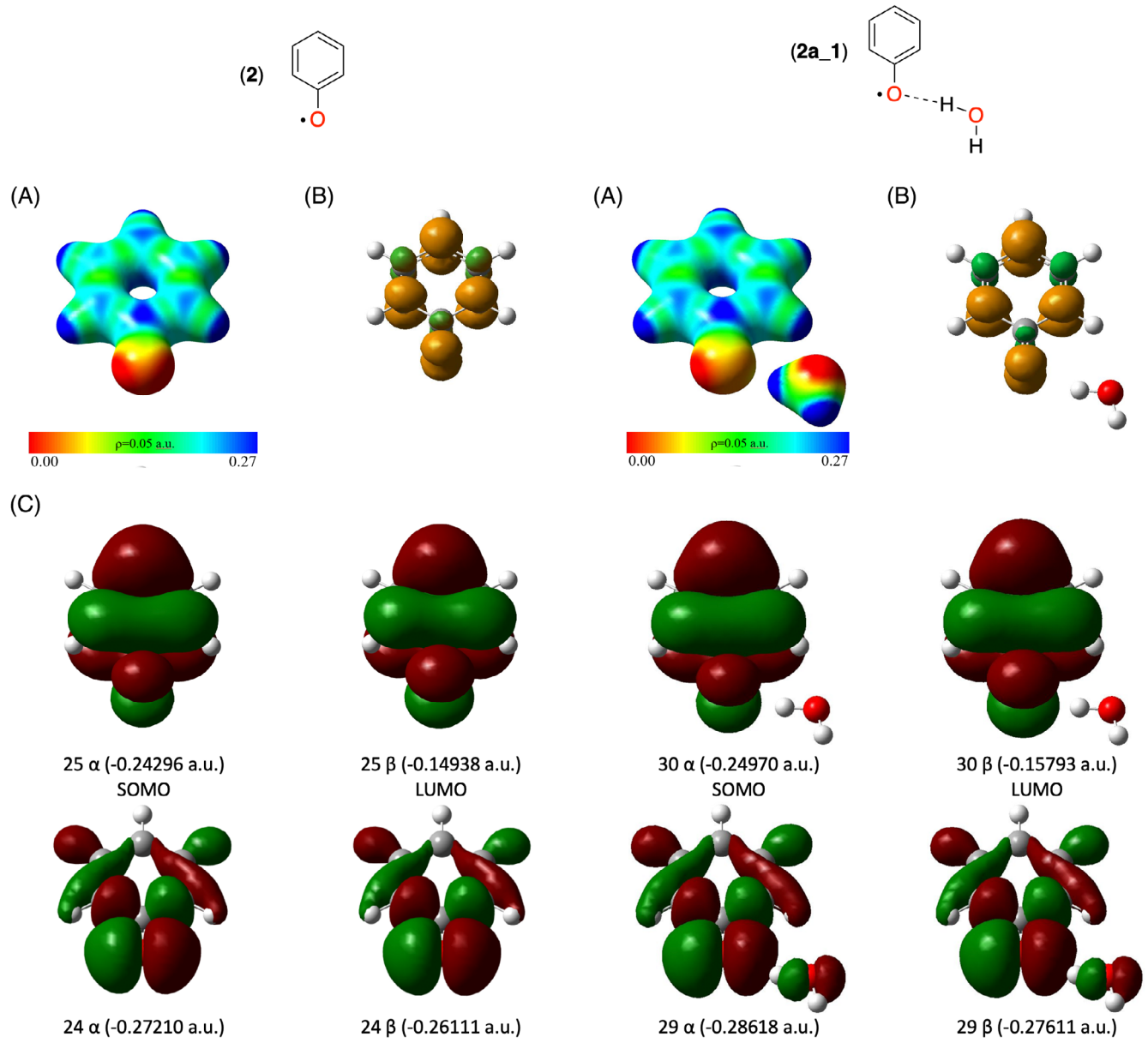

FIGURE 6 Orbital analysis for phenoxy radical (**2**) and the best conformation of its complex with one water molecule (**2a_1**). Electrostatic potential (A), spin density (SD = 0.005 a.u.) (B), and molecular orbitals (C) calculated at the UB3LYP-D3/6-31+G(d,p) level of theory.

center, is based on the concept of σ-holes as reported previously for sulfur-,[84] nitrogen-,[85] and halogen-containing compounds.[86] The electron density of the oxygen atom is slightly shifted toward the covalent bond along the C—O• (or O—O•) axis, the effect being most visible for peroxy radials.

3.4 | The effects of monosolvation on the stability of alkoxy radicals

The RSE-A values of alkoxy radicals listed in Table 2 are somewhat less negative than the RSE values in Table 1. These radicals are thus destabilized through mono-complexation with water, the destabilization varying between 2.6 kJ mol^{-1} for *n*-BuO• (**11**) and 7.0 kJ mol^{-1} for $PhCH_2O$• (**8**). These changes imply that the complexation energies for the parent alcohols (acting as H-bond acceptors) are larger than those for the respective radicals, which leads to an increase in BDE(O—H) values in the respective parent compounds (Figure 7). This may, at least in part, be due to differences in the oxygen atom partial charges (NBO), which are significantly smaller on the radical oxygen as compared to those in the parent alcohols (see Supporting Information). Changing the role of the parent alcohol to that of the H-bond donor yields the alkoxy radical RSE-D values in Table 2, which are closely similar to the RSE values of uncomplexed alkoxy radicals in Table 1. The associated BDE-D(OH) values are thus quite similar to the BDE(OH) values as shown graphically in Figure 8.

TABLE 2 RSE-A and RSE-D values (kJ mol^{-1}) calculated for selected O-centered radicals (ordered according to Table 1).

		RSE(RO•)					
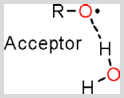		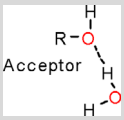 Alcohol			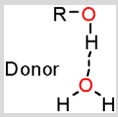 Alcohol		
Radical		DFT[a]	CBS[b]	G3B3-D3[c]	DFT[a]	CBS[b]	G3B3-D3[c]
HO•	(1)	+6.1	+4.1	+4.1[d]	+6.1	+4.1	+4.1[d]
HC(O)O•	(20)	−39.4	−10.3	−23.9 −15.0[d]	−9.0	+16.4	+3.1 +11.5[d]
t-Bu-O•	(7)	−55.1	−44.3	−44.6	−62.9	−49.5	−52.7
$PhCH_2O$•	(8)	−56.6	−45.2	−45.0	−56.5	−43.6	−44.8
CH_3O•	(6)	−60.6	−53.7	−51.6	−63.4	−55.3	−55.7
CH_3CH_2O•	(9)	−60.1	−51.5	−50.2	−65.7	−55.1	−56.1
$PhC(CH_3)_2O$•	(10)	−55.1	−41.5	−44.3	−53.5	−38.8	−40.1
n-Bu-O•	(11)	−62.7	−53.1	−52.2	−68.5	−57.1	−57.5
p-nitro-PhO•	(12)	−125.3	−115.3	−114.8	−104.7	−98.1	−95.6
HOO•	(13)	−142.9	−137.1	−137.6	−142.9	−137.1	−137.6
PhO•	(2)	−144.0	−132.5	−130.4	−133.4	−124.0	−118.9
$PhCH_2OO$•	(16)	−137.5	−126.8	−129.3	−127.5	−116.3	−118.7
CH_3OO•	(15)	−143.5	−136.0	−137.3	−132.3	−124.9	−126.1
p-methyl-PhO•	(14)	−153.1	−140.0	−138.5	−143.8	−132.7	−128.3
t-Bu-OO•	(17)	−149.6	−139.5	−144.5	−137.1	−127.8	−131.8
p-amino-PhO•	(18)	−183.2	−163.9	−165.7	−176.3	−158.2	−160.9
TEMPO•	(5)	−215.5	−203.4	−208.8	−198.6	−189.8	−191.4
•OO•	(19)				−236.4	−258.2	−257.6

[a](U)B3LYP-D3/6-31+G(d,p) level of theory.
[b]DLPNO-CCSD(T)/CBS using (U)B3LYP-D3/6-31+G(d,p) optimized geometries.
[c]Using (U)B3LYP-D3/6-31G(d) optimized geometries.
[d]Using (U)B3LYP-D3/6-31+G(d,p) optimized geometries.

Only for the benzyloxy-type radicals **8** and **19** are the RSE-D values similarly less negative than already found for the RSE-A values, the largest change being that for benzyloxy radical **8** with a ΔΔRSE = +8.6 kJ mol^{-1}.

3.5 | The effects of monosolvation on the stability of aryloxy radicals

The monosolvation enthalpy ΔH_{c1}^{gas}(ArO•) increases systematically when moving from acceptor- to donor-substituted phenoxy radicals, the lowest value being found for radical *p*-NO_2-PhO• (ΔH_{c1}^{gas}(**12**) = −20.1 kJ mol^{-1}) and the highest for *p*-NH_2-PhO• (ΔH_{c1}^{gas}(**18**) = −25.5 kJ mol^{-1}) at DLPNO-CCSD(T)/CBS level. This is accompanied by a decrease in the hydrogen bonding distances r(O•···H) of 195.2 pm for radical **12** and 183.3 pm for **18**, and an increase in the partial charge of the radical oxygen atom of −0.46 in radical **12** and −0.55 in radical **18**. It should be added that the NBO charge of the radical oxygen atom in aryloxy radicals amounts to only 70% of the charge of the same atom in the parent phenols. From a structural point of view, the aryloxy radical water complexes are largely similar in that the water is located in the aryl group ring plane. That this type of orientation provides the most effective interaction with the oxygen lone pair electron density is easily seen in Figure 6.

Comparing the RSE-A and RSE-D values for aryloxy radicals in Table 2, we note that these are actually quite different. In a very general sense, these differences result from phenols being much better hydrogen bond donors as compared to acceptors. Focusing first on the RSE-A values, we note that these are systematically larger (more negative) by approx. 10 kJ mol^{-1} as compared with the RSE values for aryloxy radicals in Table 1. This shift results from differences in complexation energies ΔH_{c1}^{gas}(ArOH) for the parent phenols, which are approx. 10 kJ mol^{-1} smaller than for the resulting phenoxy radicals. Taking the parent phenol system as an example, we have ΔH_{c1}^{gas}(**2H**) = −13.1 kJ mol^{-1} versus ΔH_{c1}^{gas}(**2**) = −21.7 kJ mol^{-1}. The difference of these values of $\Delta\Delta H_{c1}^{gas}$ = −8.6 kJ mol^{-1} is closely similar to the difference in RSE(**2**) and RSE-A(**2**) values (−123.6 vs. −132.5 kJ mol^{-1}). The range of RSE-D values listed for aryloxy radicals in Table 2 (−98.1 for radical **12** to −158.2 for radical **18**) is somewhat larger than the range of RSE values in Table 1 (from −106.1 for radical **12** to −152.4 for

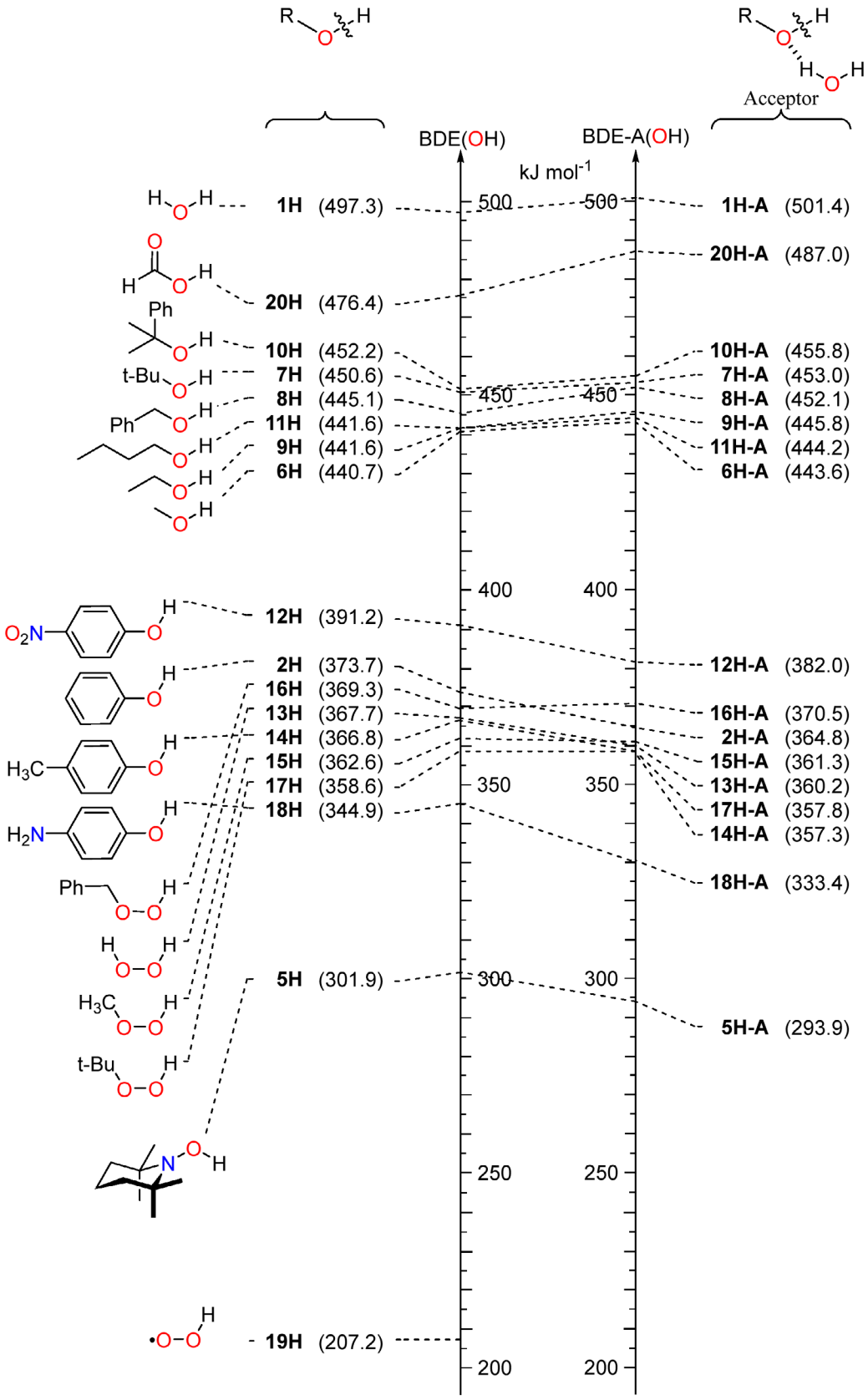

FIGURE 7 BDE(OH) and BDE-A(OH) values (DLPNO-CCSD(T)/CBS//(U)B3LYP-D3/6-31+G(d,p) results).

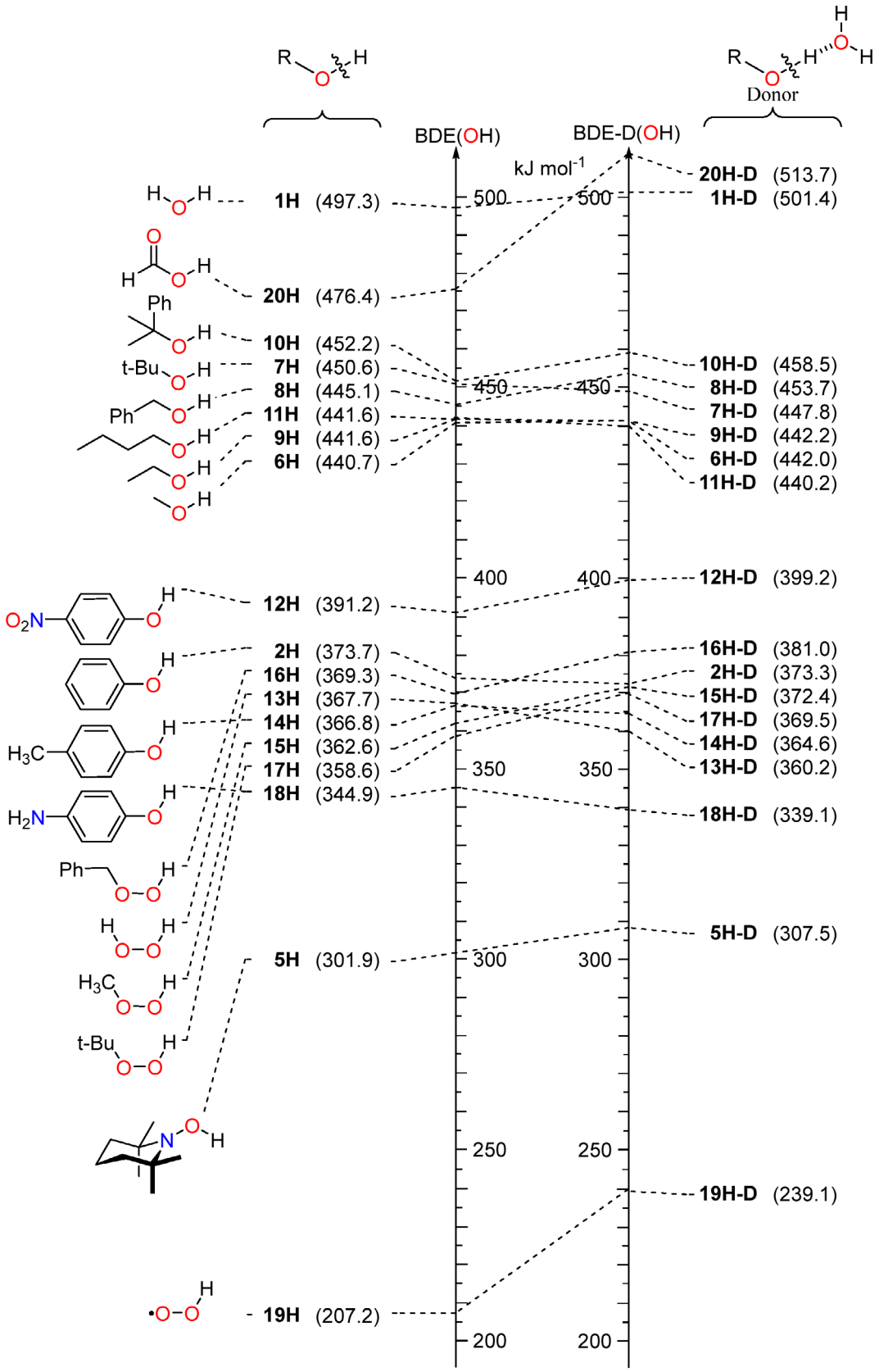

FIGURE 8 BDE(OH) and BDE-D(OH) values (DLPNO-CCSD(T)/CBS//(U)B3LYP-D3/6-31+G(d,p) results).

radical **18**). This is due to the fact that *p*-NO_2-PhOH is a much better H-bond donor as compared to the donor-substituted phenols **14H** and **18H**. As a result, we find that *p*-NO_2-PhO• is destabilized and *p*-NH_2-PhO• is (weakly) stabilized when their respective parent phenols act as H-bond donors. For the parent phenol (**2H**) system, we find that RSE and RSE-D values are almost identical (−123.6 vs.−124.0 kJ mol^{-1}).

3.6 | The effects of monosolvation on the stability of peroxy radicals, triplet dioxygen and TEMPO

The monosolvation enthalpies ΔH_{c1}^{gas}(ROO•) for the radicals CH_3OO•, *t*-BuOO•, and $PhCH_2OO$• are −13.6, −13.8, −17.0 kJ mol^{-1}, respectively. For peroxides such as CH_3OOH, *t*-BuOOH, and $PhCH_2OOH$ interacting with water as a H-acceptor ΔH_{c1}^{gas}(ROOH), these values are −13.9, −13.0, and −18.1 kJ mol^{-1}. These closely similar complexation energies of alkylperoxy radicals and alkylhydroperoxides imply that their RSE and RSE-A values are almost identical. Alkylhydroperoxides are, however, much better hydrogen bond donors than acceptors. As a consequence, the RSE-D values for alkylperoxy radicals are much smaller (less stabilizing) than the respective RSE values. For methylperoxy radical (CH_3OO•, **15**) as the smallest system in this group, the difference amounts to RSE-D = −124.9 kJ mol^{-1} versus RSE = −134.7 kJ mol^{-1}.

For HOO• (**13**) as the smallest possible peroxy radical the situation is much more complicated due to multiple interactions between the solvating water molecules and the HOO•/H_2O_2 interaction partners. The minima identified for these systems at the DLPNO-CCSD(T)/CBS//(U)B3LYP-D3/6-31+G(d,p) level of theory are shown in Figure 9 together with the respective relative stabilities. The best conformer of the HOOH···H_2O complex is of cyclic type (Figure 9A) with two H-bonds, in which the HOOH molecule can be considered as both a H-accepting(r(O_{alk}···HOH) = 227.5 pm) and a H-donating (r(OH_{alk}···OH_2) = 190.1 pm) system at the same time. The presence of two H-bonds gives this complex a rather low monosolvation enthalpy of ΔH_{c1}^{gas}(**13H**) = −22.5 kJ mol^{-1}. This type of structure was established experimentally by matrix isolation infrared spectroscopy.[87] For the HOO•···H_2O complex, we identify the three conformations shown in Figure 9E–G. The most stable conformation is also of cyclic type (Figure 9E) and is very similar to the best conformer of the HOOH···H_2O complex. In this structure, the HOO• radical is interacting with water as both a H-acceptor and a H-donor through two H-bonds: (1) between the hydrogen of water and the spin-bearing oxygen with r(O•···HOH) = 246.9 pm; and (2) between the hydrogen of the HOO• radical and the oxygen of water with r(OH_{alk}···OH_2) = 177 pm. This structure has been described already in earlier theoretical[88] and experimental[89,90] studies. The other two conformers of the HOO•···H_2O complex are more than 20 kJ mol^{-1} less stable because they contain only one H-bond with r(O•···HOH) distances of 204.6–206.4 pm as shown in Figure 9. Although the water complexes of radical **13** and its parent **13H** share large structural similarities, the complexation energy of radical **13** is significantly more favorable at ΔH_{c1}^{gas}(**13**) = −29.7 kJ mol^{-1}. This difference of 7.5 kJ mol^{-1} translates into a significant stabilization of radical **13** and the associated values of RSE(**13**) = −129.6 kJ mol^{-1} and RSE-A(**13**) = −137.1 kJ mol^{-1}. Given the simultaneous presence of multiple H-bonding interactions in the water complexes in Figure 9, RSE-A and RSE-D values are taken to be identical for this system. For triplet oxygen ($^3O_2$, **19**), the HOO• radical represents (formally) the parent alcohol. The list of conformers presented in Figure 9 for the HOO•···H_2O complex lacks a structure where the HO group oxygen interacts with water as the H-bond acceptor, and calculation of an RSE-A values is therefore impossible. Acting as a H-bond donor as in Figure 9E, radical **13** forms a much more stable water complex as compared to triplet oxygen. This leads

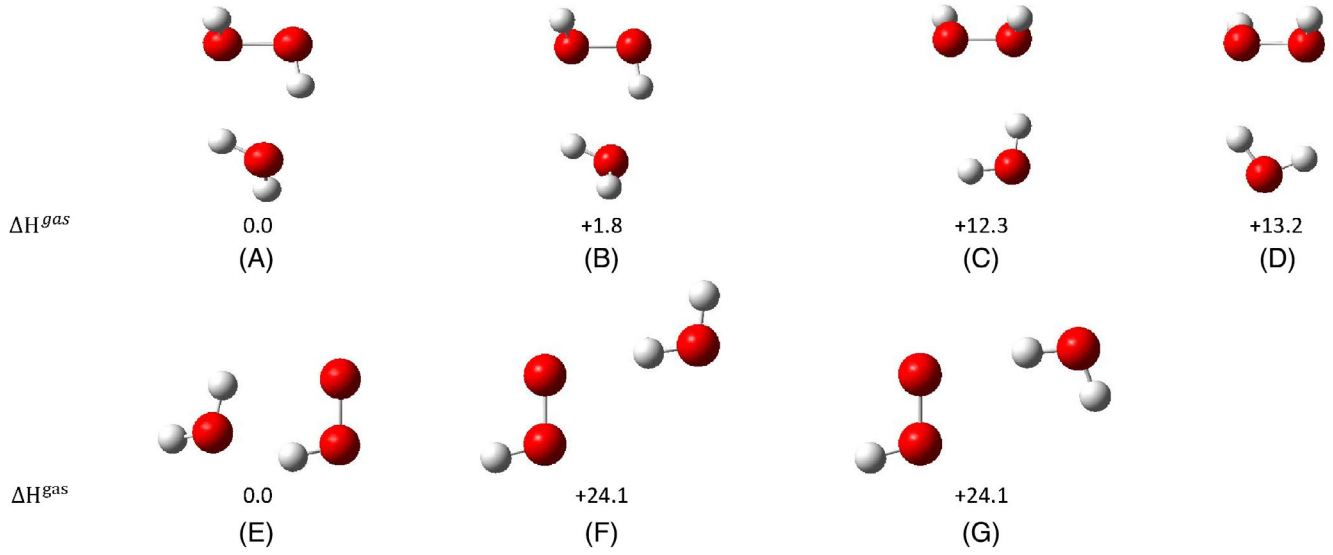

FIGURE 9 Relative ΔH^{gas} values (in kJ mol^{-1}) for the HOOH···H_2O (A–D) and HOO•···H_2O (E–G) complexes (DLPNO-CCSD(T)/CBS//(U)B3LYP-D3/6-31+G(d,p) results).

to a very substantial difference between RSE(**19**) = −290.1 kJ mol^{-1} and RSE-D(**19**) = −258.1 kJ mol^{-1}. The TEMPO radical (**5**) as the most stable (doublet) system considered here forms a water complex characterized by a comparatively short H-bond of r(O•···HOH) = 182.7 pm and a complexation energy of $\Delta H_{c1}^{gas} = -22.8$ kJ mol^{-1}. This value is larger as compared to that for the closed-shell TEMPOL parent acting as a H-bond acceptor ($\Delta H_{c1}^{gas} = -15.1$ kJ mol^{-1}), which implies that RSE-A(**5**) = −212.2 kJ mol^{-1} is more negative (more stabilizing) than RSE(**5**) = −195.4 kJ mol^{-1}. However, TEMPOL is a much better H-bond donor (than acceptor), which is also reflected in RSE-D (**5**) = −189.8 kJ mol^{-1}.

The final system considered here is HC(O)O• radical **20**, whose electronic structure varies significantly as a function of the level of theory. This is also the reason for the largely different RSE values obtained from DFT, DLPNO-CCSD(T)/CBS, and G3B3-D3 calculations (Table 1). The water complexes of formic acid (**20H**) are more stable as compared to the water complex of radical **20**, and the RSE-A and RSE-D values are thus less negative (less stabilizing) as compared to RSE(**20**) = −20.9 kJ mol^{-1}. Formic acid is a particularly good H-bond donor, which leads to RSE-D(**20**) = +16.4 kJ mol^{-1}.

4 | CONCLUSIONS

The range of (formally) oxygen-centered radicals considered here includes the comparatively unstable hydroxyl radical (**1**), alkoxy radicals such as CH_3O• (**6**), aryloxy radicals such as PhO• (**2**), peroxy radicals such as CH_3OO• (**15**), and nitroxy radicals such as TEMPO (**5**). The most favorable water complexes identified for these systems all correspond to type (A) shown in Figure 2. The alternative interaction modes described as the SEHB or 2c3e hemibond are found only in (some) higher energy conformers of the water/radical complexes. The influence of water complexation on the respective RSE values is smallest for the group of alkoxy radicals and largest for the group of aryloxy radicals. The parent alcohol system can act as H-bond donor or acceptor in almost all systems, which gives rise to the associated RSE-A and RSE-D values. The difference between BDE-A and BDE-D simply reflects the difference in hydrogen bonding in the closed shell parent. Selecting the thermochemically most stable alcohol/water complex leads to the smaller (less negative) of the RSE-A or RSE-D values. For most of the systems considered here, this is the RSE-D values, the exceptions being the alkoxy radicals CH_3O•, CH_3CH_2O•, *n*-Bu-O•, and *t*-Bu-O•.

ACKNOWLEDGMENTS

The authors thank the Deutsche Forschungsgemeinschaft (DFG, German Research Foundation) for financial support via SFB 1309 (PID 325871075). Open Access funding enabled and organized by Projekt DEAL.

DATA AVAILABILITY STATEMENT

The data that support the findings of this study are openly available in Zenodo at https://zenodo.org/.

ORCID

Vasilii Korotenko https://orcid.org/0000-0002-2045-2536

Hendrik Zipse https://orcid.org/0000-0002-0534-3585

REFERENCES

[1] J. Stubbe, W. A. van Der Donk, *Chem. Rev.* **1998**, *98*, 2661.
[2] H. Eklund, U. Uhlin, M. Färnegårdh, D. T. Logan, P. Nordlund, *Prog. Biophys. Mol. Biol.* **2001**, *77*, 177.
[3] J. Stubbe, D. G. Nocera, C. S. Yee, M. C. Chang, *Chem. Rev.* **2003**, *103*, 2167.
[4] M. Kolberg, K. R. Strand, P. Graff, K. K. Andersson, *Biochim Biophys Acta Proteins Proteom* **2004**, *1699*, 1.
[5] M. Bennati, F. Lendzian, M. Schmittel, H. Zipse, *Biol. Chem.* **2005**, *386*, 1007.
[6] J. Fritscher, E. Artin, S. Wnuk, G. Bar, J. H. Robblee, S. Kacprzak, M. Kaupp, R. G. Griffin, M. Bennati, J. Stubbe, *J. Am. Chem. Soc.* **2005**, *127*, 7729.
[7] P. Nordlund, P. Reichard, *Annu. Rev. Biochem.* **2006**, *75*, 681.
[8] H. Zipse, E. Artin, S. Wnuk, G. J. Lohman, D. Martino, R. G. Griffin, S. Kacprzak, M. Kaupp, B. Hoffman, M. Bennati, *J. Am. Chem. Soc.* **2009**, *131*, 200.
[9] A. Benjdia, K. Heil, T. R. Barends, T. Carell, I. Schlichting, *Nucleic Acids Res.* **2012**, *40*, 9308.
[10] A. C. Kneuttinger, K. Heil, G. Kashiwazaki, T. Carell, *Chem. Commun.* **2013**, *49*, 722.
[11] J. Hioe, H. Zipse, *Chem. Eur. J.* **2012**, *18*(16), 463.
[12] D. M. Chipman, *J. Phys. Chem. A* **2011**, *115*, 1161.
[13] ATcT. Active Thermochemical Tables, version 1.122p. https://atct.anl.gov.
[14] J. Hioe, H. Zipse, *Org. Biomol. Chem.* **2010**, *8*, 3609.
[15] J. Hioe, H. Zipse, *Faraday Discuss.* **2010**, *145*, 301.
[16] K. Condic-Jurkic, H. Zipse, D. M. Smith, *J. Comput. Chem.* **2010**, *31*, 1024.
[17] K. Čondić-Jurkić, V. T. Perchyonok, H. Zipse, D. M. Smith, *J. Comput. Chem.* **2008**, *29*, 2425.
[18] W. Tantawy, H. Zipse, *Eur. J. Org. Chem*, **2007**, 5817.
[19] J. Hioe, A. Karton, J. L. Martin, H. Zipse, *Chem. Eur. J.* **2010**, *16*, 6861.
[20] M. L. Coote, C. Y. Lin, H. Zipse, in *Carbon-Centered Free Radicals and Radicals Cations* (Ed: M. D. E. Forbes), John Wiley & Sons, New Jersey, USA, **2010**, p. 83.
[21] E. I. Izgorodina, D. R. Brittain, J. L. Hodgson, E. H. Krenske, C. Y. Lin, M. Namazian, M. L. Coote, *J. Phys. Chem. A* **2007**, *111*(10), 754.
[22] D. Moran, R. Jacob, G. P. Wood, M. L. Coote, M. J. Davies, R. A. O'Hair, C. J. Easton, L. Radom, *Helv. Chim. Acta* **2006**, *89*, 2254.
[23] Y. Zhao, D. G. Truhlar, *J. Phys. Chem. A* **2008**, *112*, 1095.
[24] J. Zheng, Y. Zhao, D. G. Truhlar, *J. Phys. Chem. A* **2007**, *111*, 4632.
[25] S. Grimme, *J. Chem. Phys.* **2006**, *124*, 034108.
[26] D. C. Graham, A. S. Menon, L. Goerigk, S. Grimme, L. Radom, *J. Phys. Chem. A* **2009**, *113*, 9861.
[27] D. J. Henry, C. J. Parkinson, L. Radom, *J. Phys. Chem. A* **2002**, *106*, 7927.
[28] D. J. Henry, M. B. Sullivan, L. Radom, *J. Chem. Phys.* **2003**, *118*, 4849.
[29] S. D. Wetmore, D. M. Smith, J. T. Bennett, L. Radom, *J. Am. Chem. Soc.* **2002**, *124*(14), 054.
[30] S. D. Wetmore, D. M. Smith, B. T. Golding, L. Radom, *J. Am. Chem. Soc.* **2001**, *123*, 7963.
[31] D. M. Smith, W. Buckel, H. Zipse, *Angew. Chem. Int. Ed.* **1867**, *2003*, 42.
[32] L. Curtis, K. Raghavachari, J. Pople, *J. Chem. Phys* **1993**, *98*, 1293.
[33] A. G. Baboul, L. A. Curtiss, P. C. Redfern, K. Raghavachari, *J. Chem. Phys.* **1999**, *110*, 7650.
[34] L. A. Curtiss, P. C. Redfern, K. Raghavachari, *J. Chem. Phys.* **2007**, *126*, 084108.

[35] J. A. Montgomery Jr.., M. J. Frisch, J. W. Ochterski, G. A. Petersson, *J. Chem. Phys.* **2000**, *112*, 6532.
[36] J. M. Martin, G. de Oliveira, *J. Chem. Phys.* **1843**, *1999*, 111.
[37] A. Altun, F. Neese, G. Bistoni, *Beilstein J. Org. Chem.* **2018**, *14*, 919.
[38] F. Neese, E. F. Valeev, *J. Chem. Theory Comput.* **2011**, *7*, 33.
[39] M. Saitow, U. Becker, C. Riplinger, E. F. Valeev, F. Neese, *J. Chem. Phys.* **2017**, *146*(164), 105.
[40] A. D. Becke, *J. Chem. Phys* **1993**, *98*, 5648.
[41] C. Lee, W. Yang, R. G. Parr, *Phys. Rev. B* **1988**, *37*, 785.
[42] W. J. Hehre, R. Ditchfield, J. A. Pople, *J. Chem. Phys.* **1972**, *56*, 2257.
[43] S. Grimme, S. Ehrlich, L. Goerigk, *J. Comput. Chem.* **2011**, *32*, 1456.
[44] S. Grimme, J. Antony, S. Ehrlich, H. Krieg, *J. Chem. Phys.* **2010**, *132*(154), 104.
[45] D. Šakić, M. Hanževački, D. M. Smith, V. Vrček, *Org. Biomol. Chem.* **2015**, *13*(11), 740. An interactive version of the kick script can be found at https://kick.science/KICK.html.
[46] E. Suarez, N. Diaz, D. Suarez, *J. Chem. Theory Comput.* **2011**, *7*, 2638.
[47] V. Korotenko, energy sorting script (ess), https://github.com/vnkorotenko/ess.
[48] V. Korotenko, *centroid comparison script (ccs)*. https://github.com/vnkorotenko/ccs.
[49] B. Ruscic, A. F. Wagner, L. B. Harding, R. L. Asher, D. Feller, D. A. Dixon, K. A. Peterson, Y. Song, X. Qian, C.-Y. Ng, *J. Phys. Chem. A* **2002**, *106*, 2727.
[50] K. M. Ervin, V. F. DeTuri, *J. Phys. Chem. A* **2002**, *106*, 9947.
[51] Y.-R. Luo, *Comprehensive Handbook of Chemical Bond Energies*, CRC Press, Boca Raton, **2007**.
[52] D. R. Reed, M. C. Hare, A. Fattahi, G. Chung, M. S. Gordon, S. R. Kass, *J. Am. Chem. Soc.* **2003**, *125*, 4643.
[53] A. Fattahi, S. R. Kass, *J. Org. Chem.* **2004**, *69*, 9176.
[54] T. Denisova, E. Denisov, *Kinet. Catal.* **2006**, *47*, 121.
[55] E. T. Denisov, V. Tumanov, *Russ. Chem. Rev.* **2005**, *74*, 825.
[56] R. M. Borges dos Santos, J. A. Martinho Simões, *J. Phys. Chem. Ref. Data* **1998**, *27*, 707.
[57] P. Mulder, H.-G. Korth, D. A. Pratt, G. A. DiLabio, L. Valgimigli, G. Pedulli, K. Ingold, *J. Phys. Chem. A* **2005**, *109*, 2647.
[58] M. Jonsson, *J. Phys. Chem.* **1996**, *100*, 6814.
[59] O. Kondo, S. W. Benson, *J. Phys. Chem.* **1984**, *88*, 6675.
[60] S. J. Blanksby, T. M. Ramond, G. E. Davico, M. R. Nimlos, S. Kato, V. M. Bierbaum, W. C. Lineberger, G. B. Ellison, M. Okumura, *J. Am. Chem. Soc.* **2001**, *123*, 9585.
[61] H. Wang, J. W. Bozzelli, *J. Chem. Eng. Data* **1836**, *2016*, 61.
[62] P. S. Billone, P. A. Johnson, S. Lin, J. Scaiano, G. A. DiLabio, K. Ingold, *J. Org. Chem.* **2011**, *76*, 631.
[63] L. Mahoney, G. Mendenhall, K. Ingold, *J. Am. Chem. Soc.* **1973**, *95*, 8610.
[64] M. G. Nix, A. L. Devine, B. Cronin, R. N. Dixon, M. N. Ashfold, *J. Chem. Phys.* **2006**, *125*(133), 318.
[65] M. Lucarini, P. Pedrielli, G. F. Pedulli, S. Cabiddu, C. Fattuoni, *J. Org. Chem.* **1996**, *61*, 9259.
[66] H. Zipse, *Radic Synth* **2006**, *I*, 163.
[67] J. Hioe, H. Zipse, in *Encyclopedia of Radicals in Chemistry, Biology and Materials* (Eds: C. Chatgilialoglu, A. Studer), John Wiley & Sons, Chichester, UK **2012**, p. 449.
[68] W. M. Fabian, R. Janoschek, *J. Mol. Struct. Theochem* **2005**, *713*, 227.
[69] W. T. Borden, R. Hoffmann, T. Stuyver, B. Chen, *J. Am. Chem. Soc.* **2017**, *139*, 9010.
[70] A. Mukhopadhyay, W. T. Cole, R. J. Saykally, *Chem. Phys. Lett.* **2015**, *633*, 13.
[71] A. Mukhopadhyay, S. S. Xantheas, R. J. Saykally, *Chem. Phys. Lett.* **2018**, *700*, 163.
[72] A. Engdahl, G. Karlström, B. Nelander, *J. Chem. Phys.* **2003**, *118*, 7797.
[73] J. A. Plumley, J. Dannenberg, *J. Comput. Chem.* **2011**, *32*, 1519.
[74] P. C. do Couto, R. Guedes, B. C. Cabral, J. M. Simoes, *J. Chem. Phys.* **2003**, *119*, 7344.
[75] Y. Ohshima, K. Sato, Y. Sumiyoshi, Y. Endo, *J. Am. Chem. Soc.* **2005**, *127*, 1108.
[76] S. Aloisio, J. S. Francisco, *Acc. Chem. Res.* **2000**, *33*, 825.
[77] D. P. Schofield, H. G. Kjaergaard, *J. Chem. Phys.* **2004**, *120*, 6930.
[78] Z. Zhou, Y. Qu, A. Fu, B. Du, F. He, H. Gao, *Int. J. Quantum Chem* **2002**, *89*, 550.
[79] M. P. DeMatteo, J. S. Poole, X. Shi, R. Sachdeva, P. G. Hatcher, C. M. Hadad, M. S. Platz, *J. Am. Chem. Soc.* **2005**, *127*, 7094.
[80] M. A. Allodi, M. E. Dunn, J. Livada, K. N. Kirschner, G. C. Shields, *J. Phys. Chem. A* **2006**, *110*(13), 283.
[81] U. Koch, P. L. Popelier, *J. Phys. Chem.* **1995**, *99*, 9747.
[82] S. Tsuzuki, K. Honda, T. Uchimaru, M. Mikami, K. Tanabe, *J. Am. Chem. Soc.* **2000**, *122*(11), 450.
[83] M. J. Calhorda, *Chem. Commun.* **2000**, 801.
[84] M. R. Koebel, A. Cooper, G. Schmadeke, S. Jeon, M. Narayan, S. Sirimulla, *J. Chem. Inf. Model* **2016**, *56*, 2298.
[85] R. Shukla, D. Chopra, *Phys Chem Chem Phys* **2016**, *18*(29), 946.
[86] A. Priimagi, G. Cavallo, P. Metrangolo, G. Resnati, *Acc. Chem. Res.* **2013**, *46*, 2686.
[87] A. Engdahl, B. Nelander, *Phys Chem Chem Phys* **2000**, *2*, 3967.
[88] S. Aloisio, J. Francisco, *J. Phys. Chem. A* **1899**, *1998*, 102.
[89] S. Aloisio, J. S. Francisco, R. R. Friedl, *J. Phys. Chem. A* **2000**, *104*, 6597.
[90] B. Nelander, *J. Phys. Chem. A* **1997**, *101*, 9092.

SUPPORTING INFORMATION

Additional supporting information can be found online in the Supporting Information section at the end of this article.

How to cite this article: V. Korotenko, H. Zipse, *J. Comput. Chem.* **2024**, *45*(2), 101. https://doi.org/10.1002/jcc.27221